Journal of Power Sources 195 (2010) 5417–5421

Contents lists available at ScienceDirect

Journal of Power Sources

journal homepage: www.elsevier.com/locate/jpowsour

Short communication

Preparation and electrochemical capacitance performances of super-hydrophilic conducting polyaniline

Xingwei Li*, Xiaohan Li, Na Dai, Gengchao Wang, Zhun Wang

Shanghai Key Laboratory of Advanced Polymeric Materials, Key Laboratory for Ultrafine Materials of Ministry of Education, School of Materials Science and Engineering, East China University of Science and Technology, Meilong Road 130, Shanghai 200237, PR China

ARTICLE INFO

Article history:
Received 29 September 2009
Accepted 9 March 2010
Available online 15 March 2010

Keywords:
Conducting polyaniline
Tetraethyl orthosilicate
Super-hydrophilic
Electrochemical capacitance

ABSTRACT

Super-hydrophilic conducting polyaniline was prepared by surface modification of polyaniline using tetraethyl orthosilicate in water/ethanol solution, whereas its conductivity was 4.16 S cm^{-1} at 25 °C. And its electrochemical capacitance performances as an electrode material were evaluated by the cyclic voltammetry and galvanostatic charge/discharge test in 0.1 M H_2SO_4 aqueous solution. Its initial specific capacitance was 500 F g^{-1} at a constant current density of 1.5 A g^{-1}, and the capacitance still reached about 400 F g^{-1} after 5000 consecutive cycles. Moreover, its capacitance retention ratio was circa 70% with the growth of current densities from 1.5 to 20 A g^{-1}, indicating excellent rate capability. It would be a promising electrode material for aqueous redox supercapacitors.

1. Introduction

Electrochemical capacitors, also called supercapacitors, have attracted great interest as an important energy-storage/conversion device [1,2]. Nowadays, high-surface activated carbons, noble metal oxides and conducting polymers are the main families of electrode materials for electrochemical capacitors [3–5].

Polyaniline is one of the most extensively investigated conducting polymers because of its good stability, low cost, and unique doping/de-doping mechanism [6,7]. For the electrochemical capacitor application, it is important to synthesize nano-size polyaniline, because they show better rates and larger capacities than traditional materials. Within the nano-structured electrode material, the transportation distance of ions in electrolyte is smaller than within the conventional electrode material with the same chemical composition [8–12]. Now, nano-size polyaniline with different morphologies have been synthesized by many methods [13–17], and their electrochemical capacitance performances as an electrode material have also been reported [18–22]. However, we think that super-hydrophilicity of electrode materials should also be considered for aqueous redox supercapacitors, because good hydrophilicity is advantageous to the diffusion of aqueous electrolyte during the charge/discharge process.

Here we describe an inexpensive and simple route to the preparation of super-hydrophilic conducting polyaniline by surface modification of polyaniline using tetraethyl orthosilicate in water/ethanol solution. What is particularly exciting is that the surface modification enables the formation of abundant mesopores in polyaniline, which contributes excellent electrochemical capacitance performances to polyaniline electrode material. The electrochemical investigations show that its specific capacitance is 500 F g^{-1} at a constant current density of 1.5 A g^{-1} in 0.1 M H_2SO_4 aqueous solution, and the capacitance retention ratios reaches circa 70% with the growth of current densities from 1.5 to 20 A g^{-1}. It would have a great potential for aqueous redox supercapacitors application.

2. Experimental

Aniline (Shanghai Chemical Works, China) was redistilled before use, while tetraethyl orthosilicate (Shanghai Medical and Chemical Works, China) was used without further purification. Other chemicals used were of analytical reagent grade.

Preparation of conducting polyaniline (PAn) was shown as follows. First, 0.9 ml of aniline was injected into 80 ml of 1.5 M HCl, and then 2.28 g of $(NH_4)_2S_2O_8$ (APS) (dissolved in 20 ml of de-ionized water) was quickly added into above solution. The mixture was kept stirring for 5 h at room temperature. The product was filtered, and washed with de-ionized water until the filtrate became colorless and neutral. Undried polyaniline (contained 80% water) was obtained.

Super-hydrophilic conducting polyaniline (SH-PAn) was prepared as follows. 22 ml of tetraethyl orthosilicate (TEOS) was mixed with 22 ml of anhydrous ethanol, and then 6 g of undried

* Corresponding author. Tel.: +86 21 64253527; fax: +86 21 64251372.
E-mail address: lixingwei_nj@yahoo.com (X. Li).

0378-7753/$ – see front matter © 2010 Elsevier B.V. All rights reserved.
doi:10.1016/j.jpowsour.2010.03.034

polyaniline was dispersed in above solution under ultrasonication. After the pH value of the suspended liquid was adjusted to 3 with 1.5 M HCl, de-ionized water was added, and the final mole ratio of H_2O and TEOS was 3 to 1. The hydrolysis and condensation of TEOS were carried out for 24 h under constant stirring at 25 °C. Product was filtrated, and washed with de-ionized water. Finally, it was dried at 60 °C for 24 h under vacuum. A fine green powder was obtained.

The process of hydrolysis and condensation of TEOS is described as follows:

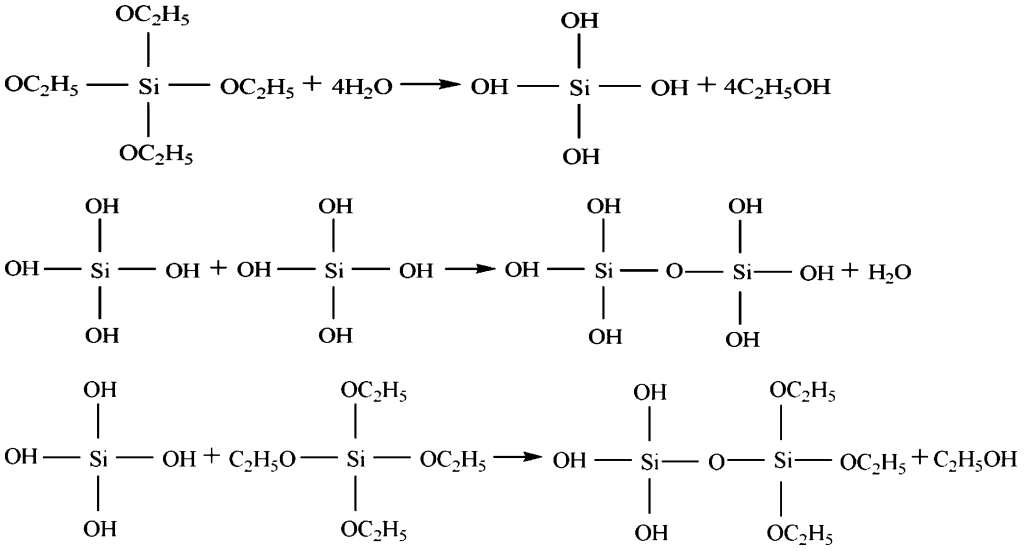

PAn-based and SH-PAn-based working electrodes were prepared as follows: the mixtures containing 75 wt% PAn or SH-PAn, 20 wt% Super P and 5 wt% polyvinylidene fluoride were well mixed, and then the mixture was spread onto carbon paper substrate, which its area was circa 0.5 cm^2.

The electrochemical performances of working electrode were characterized by a CHI760C potentiostat/galvanostat at 25 °C. A conventional three-electrode cell was used, in which platinum and the saturated calomel electrode (SCE, 0.242 V vs. the normal hydrogen electrode (NHE)) were used as counter and reference electrodes, respectively. The constant current charge/discharge cycling was performed by a Land CT 2001A battery workstation at 25 °C within the potential window 0–0.80 V vs. SCE. The used electrolyte was 0.1 M H_2SO_4 aqueous solution.

Fourier-transform infrared spectra (FTIR) of the powder samples were recorded with a Nicolet Magna IR550 spectrometer. The component analysis for SH-PAn was done by a scanning electron microscopy equipped with an energy dispersive X-ray system (SEM/EDS) (SEM: JSM-6360LV, EDS: Falcon). And the morphology was also observed by a JSM-6360LV scanning electron microscope. Measurements of wide-angle X-ray diffraction (WXRD) were carried out on a Rigaku D/Max 2550 VB/PC X-ray diffractometer using Cu K_α radiation. BET specific surface, average pore size and pore size distributions were measured by a ST-08A Surface Area and Pore Size Analyzers. The contact angles of samples were measured with a JC2000A static contact angle/surface tension analyzer at 25 °C. Conductivities were measured on compressed pellets of powder sample by the conventional four-probe technique at 25 °C.

3. Results and discussion

3.1. Morphology and surface properties

SEM and contact angles of SH-PAn and PAn are given in Fig. 1. Fig. 1 shows that SH-PAn is irregular granule. Comparing Fig. 1a with c, it is obvious that the morphology of PAn has some changes after the surface modification. However, the contact angle of SH-PAn for aqueous solution is 0°, indicating that SH-PAn is of superhydrophilicity, and the contact angle of PAn is about 81°.

In order to investigate the effects of the surface modification on surface area, average pore size and pore size distributions, BET specific surface, BJH adsorption average pore diameter and pore size distributions of SH-PAn and PAn are also measured, which results are shown in Tables 1 and 2. It is obvious that BET specific surface of SH-PAn, which is 178.3549 $m^2 g^{-1}$, is larger than that of PAn (27.5698 $m^2 g^{-1}$), and BJH adsorption average pore diameter of SH-PAn is 3.5846 nm, which is far smaller than that of PAn (26.8780 nm). This suggests that TEOS polycondensate should be modified on the surface of PAn, and large numbers of mesoporous are created, which endow SH-PAn with high specific surface.

3.2. Conductivity

The conductivity of SH-PAn reaches 4.16 S cm^{-1} at 25 °C, which is on the same order of magnitude in comparison with that of PAn (6.87 S cm^{-1}). This also indicates that TEOS polycondensate does not form a compact wrap, which is likely to form an enclosing open-work structure, or else the conductivity of SH-PAn should greatly decrease.

Table 1
Specific surface, average pore diameter of SH-PAn and PAn.

Specific surface and average pore diameter	SH-PAn	PAn
BET specific surface ($m^2 g^{-1}$)	178.3549	27.5698
BJH adsorption average pore diameter (nm)	3.5846	26.8780

Table 2
The pore size distributions of SH-PAn and PAn.

Pore size range (nm)	SH-PAn (%)	PAn (%)
<5	78.99	4.03
5–30	4.35	18.17
30–50	2.36	15.49
50–100	5.25	27.11
>100	9.05	35.20

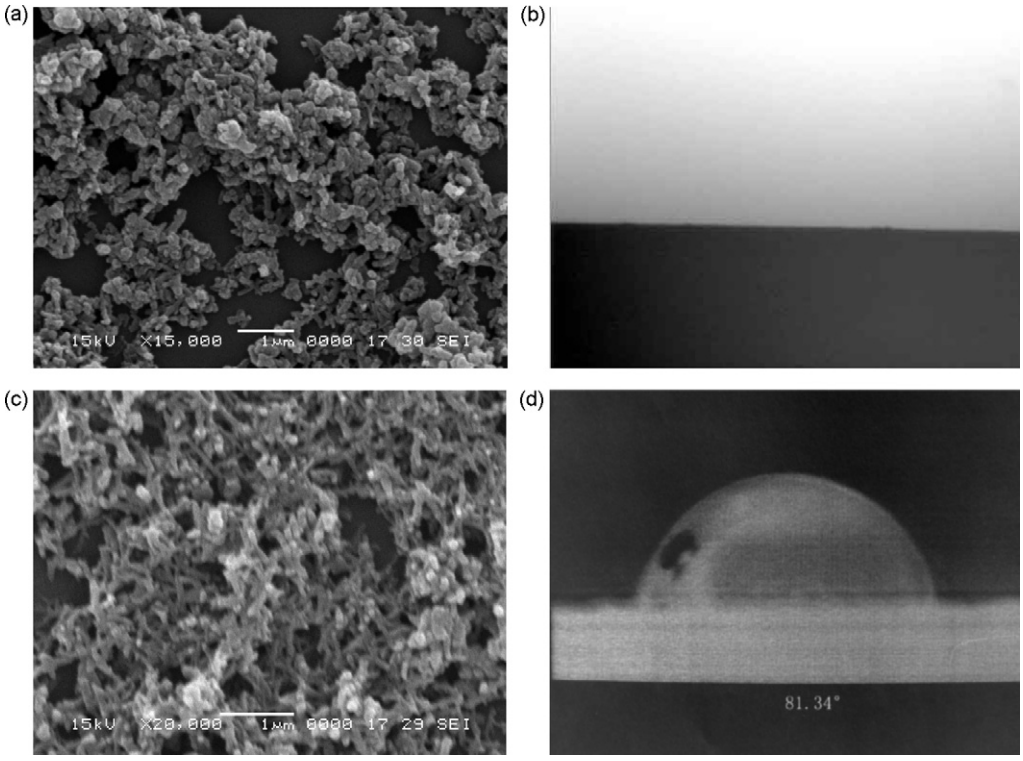

Fig. 1. SEM and contact angles of SH-PAn (a and b) and PAn (c and d), aqueous solution is used as wetting agent.

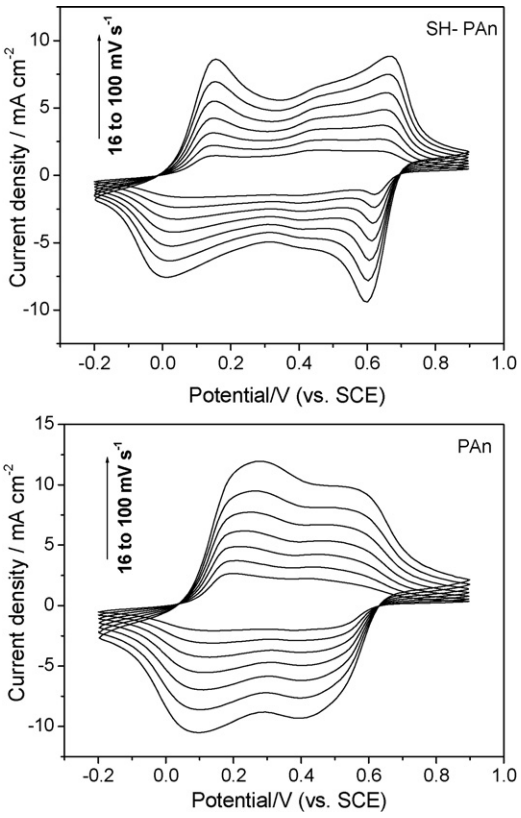

Fig. 2. CVs of SH-PAn and PAn at different scan rates (16, 25, 36, 49, 64, 81 and 100 mV s^{-1}), electrolytic solution: 0.1 M H_2SO_4 aqueous solution.

3.3. Electrochemical capacitance performances

CVs of SH-PAn and PAn at different scan rates are given in Fig. 2, which are 16, 25, 36, 49, 64, 81 and 100 mV s^{-1}, respectively. Fig. 2 shows that the capacitance characteristics of SH-PAn-based and PAn-based electrodes are distinct from that of the electric double-layer capacitance, which produces a CV curve close to the ideal rectangular shape. From Fig. 2, it is also noted that the redox currents of SH-PAn and PAn clearly increase with increasing scan rate. The slight shifts of redox peaks are observed with an increase of scan rate, but they still indicate good rate capability.

Electrochemical capacitance performances of SH-PAn are summarized in Figs. 3 and 4. Fig. 3a gives the charge/discharge curves of SH-PAn at different current densities (1.5, 2.5, 5.0, 7.5, 10, 12.5, 17.5, 15, 20 A g^{-1}) within a potential window 0–0.7 V vs. SCE. Their specific capacitance can be calculated according to the fowling formula [23].

$$C_m = \frac{C}{m} = \frac{I \times t}{\Delta V \times m}$$

where C_m is the specific capacitance [F g^{-1}], I is charge/discharge current, t is the time of charge/discharge, ΔV is the voltage difference between the upper and lower potential limits, and m is the mass of active material.

Although the capacitance of SH-PAn slowly decreases with the growth of current density, as shown in Fig. 3b, the capacitance retention rate still reaches circa 70% with growth of current densities from 1.5 to 20 A g^{-1}, indicating that high capacitance of SH-PAn-based electrode can be maintained under high power operations.

The specific capacitance as a function of cycle numbers is given in Fig. 4. Fig. 4 shows that the specific capacitance of SH-PAn-based electrode material is about 500 F g^{-1} in the initial cycle, and still retains 80% (circa 400 F g^{-1}) after 5000 consecutive cycles. This means that SH-PAn-based electrode material has also good cycle stability during the charge/discharge process.

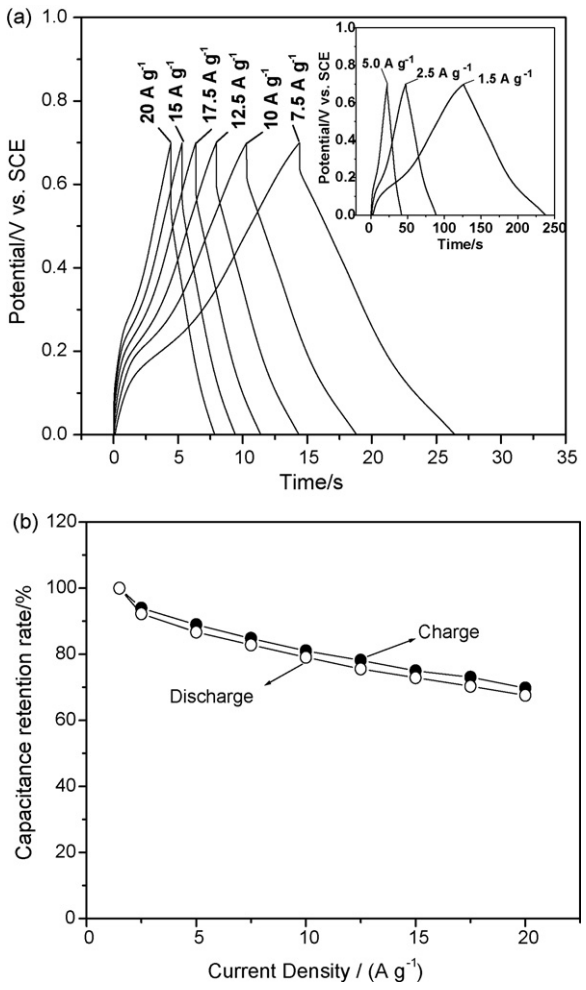

Fig. 3. (a) Charge/discharge tests of SH-PAn with various currents (1.5, 2.5, 5.0, 7.5, 10, 12.5, 17.5, 15, 20 A g^{-1}) and (b) capacitance retention rate vs. charge/discharge current density.

Good electrochemical capacitance performances of SH-PAn-based electrode material should owe to the presence of mesoporous structure and its super-hydrophilicity. First, plentiful mesoporous and super-hydrophilicity provide a fast and short diffusion approach for the aqueous electrolyte. During the charge/discharge process, the diffusion length L of ions within the electrode can be estimated as $(Dt)^{1/2}$, where D and t are the diffusion coefficient and time, respectively [4]. The value of t decreases rapidly at high charge/discharge current density. Therefore, increasing the diffusion coefficient (D) and reducing the diffusion length (L) will ensure the high utilization of electrode materials. Second, large numbers of mesoporous endow SH-PAn with high specific surface, which make actual current density in SH-PAn-based electrode material decrease. Consequently, the degradation of polyaniline due to high overpotential is reduced. Moreover, an enclosing openwork structure built by TEOS polycondensate can relieve the changes of polyaniline volume due to the inset/out of ions during the charge/discharge process, especially at high current densities. It is also advantageous for improving the electrochemical cycle stability of polyaniline.

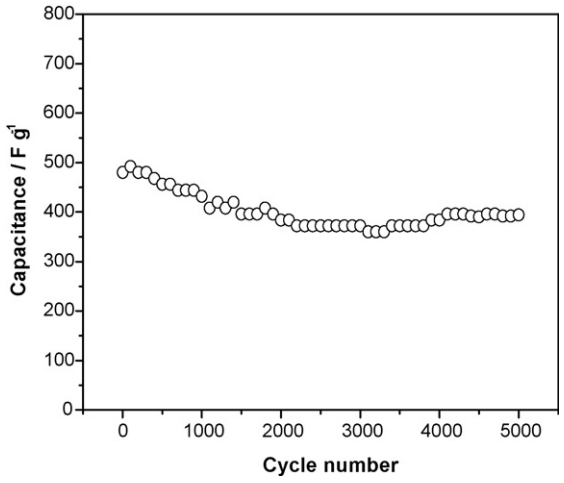

Fig. 4. Capacitance of SH-PAn vs. cycle number, charge/discharge at a current densities of 1.5 A g^{-1} within the potential window 0–0.8 V vs. SCE.

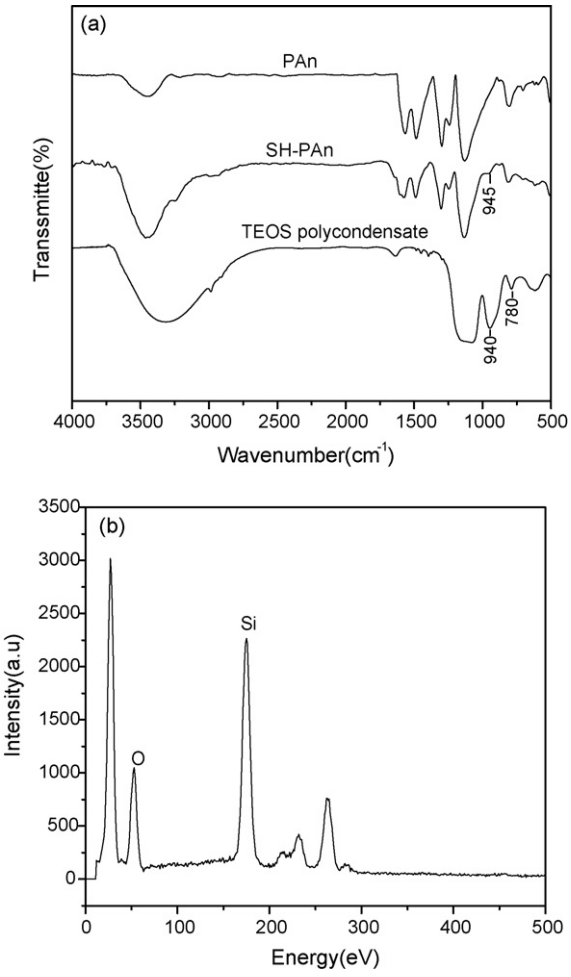

Fig. 5. (a) FTIR spectra of SH-PAn and PAn and (b) EDS of SH-PAn.

3.4. Fourier-transform infrared spectra and energy dispersive spectroscopy

The occurrence of hydrolysis and condensation of TEOS is also confirmed by FTIR spectra and EDS, as shown in Fig. 5. In the FTIR spectrum of TEOS polycondensate, there is a peak at 940 cm^{-1} coming from the stretching vibration of Si–OH group, a width peak at 3000–3600 cm^{-1} is attributed to –OH group asymmetric stretching, and the peaks at 1000–1100 cm^{-1} is assigned to Si–O–Si asymmetric stretching, while Si–O–Si symmetric stretching is about at 780 cm^{-1} [24–26]. Comparing with FTIR spectra of PAn and SH-PAn, it is noted that the peak related –OH group asymmetric stretch-

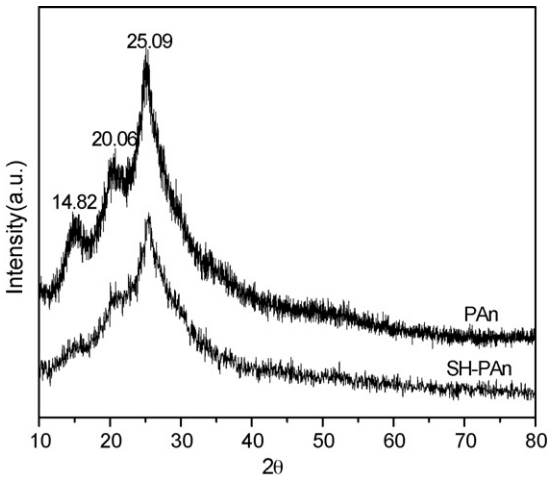

Fig. 6. Wide-angle X-ray diffraction of SH-PAn and PAn.

ing has changes. Although the peak at 1000–1100 cm^{-1} assigned to Si–O–Si asymmetric stretching is covered by other strong peaks coming from PAn, EDS of SH-PAn clearly suggests the presence of silicon in the reaction product, as shown in Fig. 5b. Moreover, the stretching vibration of Si–OH group is also found. Therefore, it is believed that TEOS polycondensate is formed, accompanying by the hydrolysis and condensation of TEOS.

3.5. Wide-angle X-ray diffraction

Wide-angle X-ray diffraction patterns for PAn and SH-PAn are given in Fig. 6. In the pattern of PAn, there are three broad peaks centered at $2\theta = 14.82^\circ$, 20.06° and 25.09°, which are ascribed to the periodicity parallel and perpendicular to the polyaniline chain, respectively [27,28]. Fig. 6 shows that the diffraction pattern of SH-PAn is similar to that of PAn, whereas the amorphous region is dominant. However, diffractive peaks at 14.82° and 20.06° hardly disappear in SH-PAn. This means that the arrangement of polyaniline chain also has slight changes in the process of the surface modification, whereas the periodicity perpendicular is of predominance absolutely in SH-PAn.

4. Conclusion

A novel method is found to prepare polyaniline with good electrochemical capacitance performances for aqueous redox supercapacitors. TEOS polycondensate endows polyaniline with super-hydrophilic property and creates plentiful mesoporous structures, which provide a fast and short diffusion approach for the aqueous electrolyte. As an electrode material, it shows large specific capacitance, high rate capability and good cycle stability in 0.1 M H_2SO_4 aqueous solution. Its specific capacitance is 500 $F g^{-1}$ at a constant current density of 1.5 $A g^{-1}$, and the capacitance retention ratios reaches circa 70% with the growth of current densities from 1.5 to 20 $A g^{-1}$. The method we used is very simple, and it is probably more practical to bring about industrialization.

Acknowledgements

We are grateful for the financial support from the Shanghai Municipal Science and Technology Commission (0852nm02000), Shanghai Leading Academic Discipline Project (B502) and Shanghai Key Laboratory Project (08DZ2230500).

References

[1] S. Sarangapani, B.V. Tilak, C.P. Chen, J. Electrochem. Soc. 143 (1996) 3971.
[2] Y.G. Wang, Z.D. Wang, Y.Y. Xia, Electrochim. Acta 50 (2005) 5641.
[3] W. Sugimoto, H. Iwata, Y. Yasunaga, Y. Murakami, Y. Takasu, Angew. Chem. Int. Ed. 42 (2003) 4092.
[4] Y.G. Wang, H.Q. Li, Y.Y. Xia, Adv. Mater. 18 (2006) 2619.
[5] D.W. Wang, F. Li, M. Liu, G.Q. Lu, H.M. Cheng, Angew. Chem. Int. Ed. 47 (2008) 373.
[6] E.T. Kang, K.G. Neoh, K.L. Tan, Prog. Polym. Sci. 23 (1998) 277.
[7] A.G. MacDiarmid, Angew. Chem. Int. Ed. 40 (2001) 2581.
[8] Y. Sato, K. Yomogida, T. Nanaumi, K. Kobayakawa, O. Yasuhiko, M. Kawai, Electrochem. Solid State Lett. 3 (2000) 113.
[9] F.S. Cai, G.Y. Zhang, J. Chen, X.L. Gou, H.K. Liu, S.X. Dou, Angew. Chem. Int. Ed. 116 (2004) 4308.
[10] X.X. Li, F.Y. Cheng, B. Guo, J. Chen, J. Phys. Chem. B 109 (2005) 14017.
[11] D.L. Li, H.S. Zhou, I. Honma, Nat. Mater. 3 (2004) 65.
[12] H.S. Zhou, D.L. Li, M. Hibino, I. Honma, Angew. Chem. Int. Ed. 44 (2005) 797.
[13] Z.M. Zhang, Z.X. Wei, M.X. Wan, Macromolecules 35 (2002) 5937.
[14] J.X. Huang, R.B. Kaner, J. Am. Chem. Soc. 126 (2004) 851.
[15] J.X. Huang, Pure Appl. Chem. 78 (2006) 15.
[16] M.X. Wan, Adv. Mater. 20 (2008) 2926.
[17] X.W. Li, X.H. Li, N. Dai, G.C. Wang, Appl. Surf. Sci. 255 (2009) 8276.
[18] K.S. Ryu, K.M. Kim, N.G. Park, Y.J. Park, S.H. Chang, J. Power Sources 103 (2002) 305.
[19] E. Frackowiak, V. Khomenko, K. Jurewicz, K. Lota, F. Bĭeguin, J. Power Sources 153 (2006) 413.
[20] X. Zhang, L.Y. Ji, S.C. Zhang, W.S. Yang, J. Power Sources 173 (2007) 1017.
[21] S.R. Sivakkumar, W.J. Kim, J.A. Choi, D.R. MacFarlane, M. Forsyth, D.W. Kim, J. Power Sources 171 (2007) 1062.
[22] H. Zhang, G.P. Cao, Z.Y. Wang, Y.S. Yang, Z.J. Shi, Z.N. Gu, Electrochem. Commun. 10 (2008) 1056.
[23] Y.G. Wang, Y.Y. Xia, J. Electrochem. Soc. 153 (2006) A450.
[24] Y.J. Wang, X.H. Wang, J. Li, Z.S. Mo, X.J. Zhao, X.B. Jing, F.S. Wang, Adv. Mater. 13 (2001) 1582.
[25] X. Zhang, Y.Y. Wu, S.Y. He, D.Z. Yang, Surf. Coat. Technol. 201 (2007) 6051.
[26] X.W. Li, N. Dai, S.R. Pan, G.C. Wang, J. Colloid Interface Sci. 322 (2008) 429.
[27] Y.S. Yang, M.X. Wan, J. Mater. Chem. 12 (2002) 897.
[28] J.P. Pouget, M.E. Jdzefowiczt, A.J. Epstein, X. Tang, A.G. MacDiarmid, Macromolecules 24 (1991) 779.